



# Study and application of a continuous inversion model of coal seam gas pressure in front area of heading face

Longyong Shu<sup>1</sup> · Yankun Ma<sup>1</sup> · Zhengshuai Liu<sup>1</sup> · Hongyan Li<sup>1</sup>

Received: 20 October 2022 / Revised: 15 June 2023 / Accepted: 10 August 2023  
© The Author(s) 2023

## Abstract

The gas pressure in front area of heading face is essential to dynamically evaluate coal and gas outburst during coal mining. In this work, a novel inversion model of gas pressure in front area of the heading face was established on premise of the hypothesis that a time-dependent zone of steady flow exists within newly exposed face. The key parameters in the inversion model were obtained based on the gas emission models and field data of gas emission rate in different times, which were used to calculate the volumes of gas emission from different sources. The results show that the percentage of gas emission from the heading face, coal wall and collapsed coal ranges from 7% to 47%, 47% to 82% and 2% to 11%, respectively. Based on the calculated volumes of gas emission and gas pressure inversion model, the gas pressure was obtained and transformed to the gas content. The absolute errors between the gas content tested and transformed in every hour is 0.4%–33%, which proved the rationality of gas pressure inversion model. Furthermore, the daily drifting footage, the radius of gas pressure boundary and the gas permeability coefficient of coal seam were confirmed to have a great effect on the result of gas pressure inversion. The inversion results verify that the speedy excavation can increase the risk of coal and gas outburst. This work produces a useful method for gas disaster prevention and control that converts the gas emission rate to an index of gas pressure within coal seam.

**Keywords** Gas disaster · Gas pressure · Inversion model · Gas emission · Heading face

## 1 Introduction

Currently, massive coal mines in China suffer the risk of gas disaster, which seriously threatens the safety of personnel and coal mines (Ma et al. 2020; Wang et al. 2020a). The gas pressure, supposed as the main driving force of gas migration in coal seam, is used as one of the indicators for an instantaneous outburst of coal and gas. The measuring results of gas pressure in coal seam influence the assessment of actual gas occurrence and division of outburst area. The quality and quantity of measuring points plays an important role on the reasonable plan of auxiliary operations for coal mining, such methods of gas drainage, periods of gas extraction and coalface heading. Therefore, the measurement of

gas pressure within coal seam is an important step to evaluate the severity of gas disasters in new mining areas as well as gas content.

At present, the measuring methods of gas pressure in coal seam include direct method and indirect method. The direct method requires drilling a borehole reaching the measuring spot of coal seam. The releasing gas is sealed in borehole, which makes pressure rise and steady. Periods of gas pressure stabilization are related to the factors of gas flow in coal seam, such as geo-stress, fractures distribution, gas content and filtration capacity (Khristianovich and Kovalenko 1988; Zhang et al. 2016). The difference of most direct methods is the borehole sealing technology, including materials, the number of plugs and grouting method (Wang et al. 2020b; Kurlenya et al. 2014; Zhang et al. 2019). The typical technological process is named “two-plug and one-grout” in China, as shown in Fig. 1. The emission gas is sealed by sealing materials between the plugs in borehole, such as expanding cement and cement mortar. The pressure values are observed from the pressure gauges, which will be steady after 10 to 30 days. For the direct method, a large number of boreholes

✉ Longyong Shu  
slyccri@163.com

✉ Yankun Ma  
yankunma@163.com

<sup>1</sup> China Coal Research Institute, Beijing 100013, China

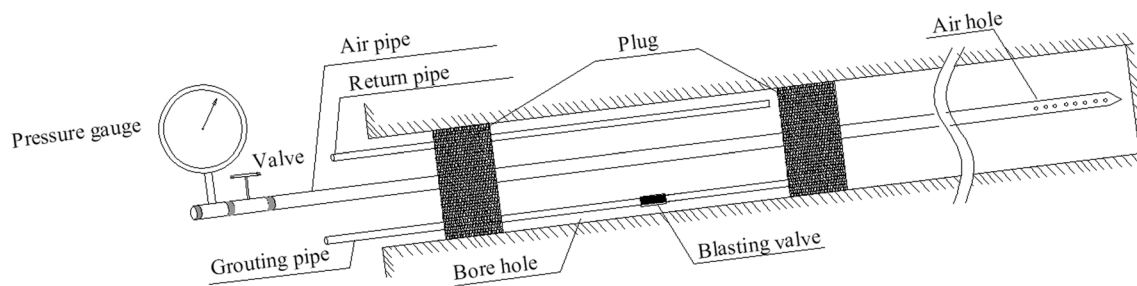


**Fig. 1** Method of gas pressure measuring underground coal mine

need to be constructed, and a limited number of results are obtained for the test area, resulting in high cost and huge quantities of engineering.

To overcome the shortcomings of the direct method, scholars have developed the indirect method, which uses geophysical exploration and theoretical calculation to predict gas pressure. Statistical analysis of gas pressure in coal seams is feasible and popular in China. Wang et al. (Wang et al. 2012) proposed a safety-line method for relationship between gas pressure and depth to predict deep coal-seam gas pressure. Wu et al. (Wu et al. 2006) obtained a power function relationship between the residual gas content and gas pressure through experiment results. Zhang et al. (2021) adopt the multiple linear regression to predict gas pressure of coal seam by building relationships among the burial depth, thickness, coal structure index and structural curvature. The geophysical exploration technology is also used by scholars to study coal gas reservoirs, such as 3D seismic fine interpretation technique (Shi et al. 2018), amplitude variation with offset (Peng et al. 2006), and transient electromagnetic (Wang et al. 2017). The geophysical methods have a high degree of explanation to gas pressure and content in coal seams. In addition, theoretical calculation method based on gas flow rules was used to analyze gas pressure values in coal face. Wang et al. (1999) proposed a one-dimensional stable gas flow equation to calculate coal bed gas pressure. Gas flow in coal body is simulated to analyze pressure changes and distributions (Valliappan and Zhang 1996; Zhao et al. 2004; Liu et al. 2018). An et al. (2011) developed a method to determine gas pressure based on gas desorption characteristics. Wang et al. (Wang et al. 2021) used an inversion model of gas pressure to predict the pressure values in coal seam based on directional drill technology. Compared with the direct method, indirect method can obtain pressure changes and distribution rapidly but with lower accuracy. Although the research on the pressure measurement with the indirect method has made great process, few studies focused on the inversion of gas pressure based on gas emission in process of tunneling. Gas volumes emitting from coal body can be monitored by sensing system (Dougherty and Özgen Karacan 2011; Zhou et al. 2020) and described

by theoretical modeling (Wang et al. 2021; Karacan et al. 2011). The gas pressure can be continuously inverted and modified by a calculation model, which should be deeply investigated.

In this work, a dynamic inversion model of gas pressure is established in front area of the heading face based on gas emission volumes from different sources (newly exposed coal in the heading face, coal wall and collapsed coal) and theoretical models. Characteristics of gas seepage and emission attenuation are analyzed in terms of physics and mathematics. By monitoring gas emission volumes and daily drifting footage of heading face, the model was applied to continuously obtain the gas pressure in front area of the heading face. The calculated gas pressure was transformed to the gas content, which was used to verify the inversion model by comparing the gas content tested. The research proposes a novel measuring method of gas pressure and has an important and practical significance for prevention and control of coal and gas outburst.

## 2 Theoretical analysis and model construction

### 2.1 Gas emission source of an excavating roadway

#### 2.1.1 Gas sorption and release in coal seam reservoirs

Coal-natural gas system is described by sorption and release in coal seam reservoirs. Coal-bed gas is deposited in coal in two forms: one is gas adsorbed in micro-pores, coal molecular structure and on larger pore surface; the other is free gas in meso-pores and macro-pores (Ceglarska-Stefanska and Zarębska 2005; Czerw 2011). Macro-pores are distributed in coal but limited in number. Micro-pores account for a considerable volume and contribute most of the total specific surface area, implying the great gas adsorption capacity (Hou et al. 2017; Zhao et al. 2016). As pore pressure reduces, gas desorbs from pore surfaces and propagates towards the macro-pores or fractures. Gas release is highly dependent on porosity of the macro-pore network.

Micro-pores in coal show low connectivity and absence of filtration capacity (Khodot et al. 1972; Zhao et al. 2018; Gerami et al. 2016). Coal seam reservoirs behave low permeability and a restricted efficiency of gas drainage in colliery. All this adds up to a concept of “bottleneck” for gas recovery.

The concept of “bottleneck” indicates that gas migration in macro-pores or fractures, including free gas and small amount of desorbing gas, is driven by gas pressure of coal. During underground coal mining, the gas emission rate in a borehole or roadway is characterized by a significant initial value and continuous decay over time. These phenomena can be explained by the concept of bottleneck.

### 2.1.2 Gas emission of an excavating roadway

Gas emission of an excavating roadway comes from the heading face, coal wall and collapsed coal. The volumes of gas emission in an excavating roadway can be expressed by Eq. (1).

$$Q = Q' + Q'' + Q''' \tag{1}$$

where  $Q$  is the total volumes of gas emission in roadway,  $Q'$ ,  $Q''$  and  $Q'''$  are the volumes of emission gas from heading face, coal wall and collapsed coal respectively.

Figure 2 shows the normal ventilation and CH<sub>4</sub> sensor locations in roadway. Gas concentration in heading face is monitored by sensor T1 and used for the warning of gas overrun. The sensor T2 in air outlet can be used for monitoring volumes of gas emission, as the return air without obstacles is basically in constant flow rate. Furthermore, the monitored results can accurately show whether the face is in production and the regularity of gas emission in work face.

Figure 3 shows the variation of CH<sub>4</sub> concentration in heading face when the ventilation breaks down. Damaged ventilation results in few air flow in head face and the volumes of CH<sub>4</sub> can be monitored by T2. The gas emissions increase steadily in 30 or 40 min later.

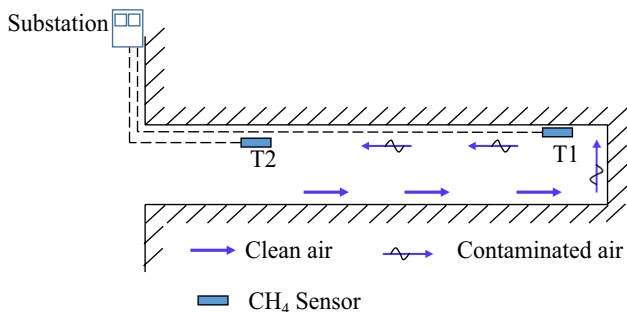


Fig. 2 Location of CH<sub>4</sub> sensors and air flow in roadway (“T1” stands for location of heading face; “T2” stands for location of air outlet)

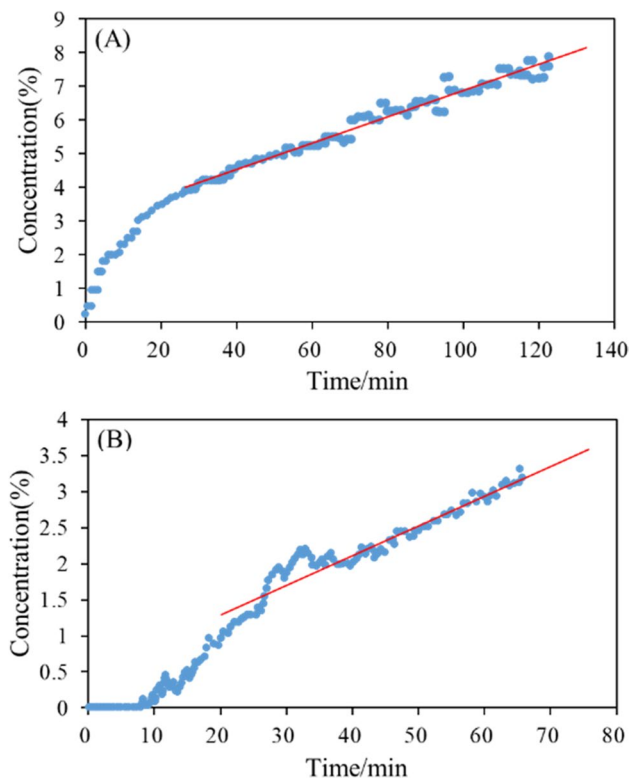


Fig. 3 Variation of CH<sub>4</sub> concentration in heading face when the ventilation breaks down a The air blower is stopped in Yuyang Colliery b The ventilation duct is disconnected in Xinzhuang Colliery

According to the results of gas migration simulation by An et al. (Fig. 4) (An et al. 2013), the scope of gas pressure distribution in front of heading face almost does not change in a certain time. Gas in fracture discharges quickly and in coal matrix creates smaller pressure gradient. The priority of gas migration in coal seam is the gas stored in fractures or macro-pores. In view of the theoretical

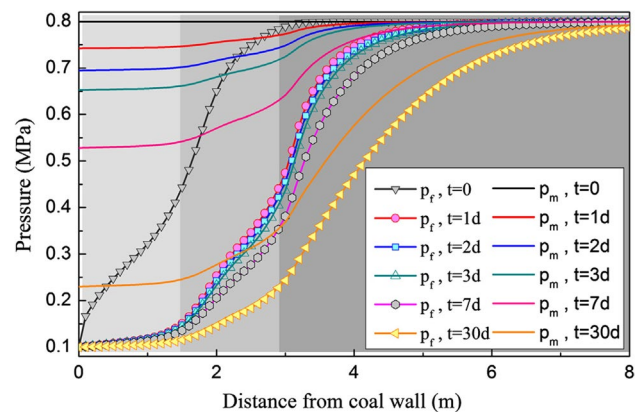


Fig. 4 Gas pressure distribution of coal fractures and matrix (An et al. 2013)

analysis and observations on-sites, an attempt is made below to explain the regularity of gas emission. The gas emission from newly exposed coal body is driven by coal seam gas pressure, and gas seepage is close to steady flow within a period.

## 2.2 Gas emission model for the sources

### 2.2.1 Gas emission model of heading face

Based on the concept of bottle neck and the specific phenomena of gas emission from the newly exposed coal body (in Sect. 2.1), the following physical laws and hypotheses are taken to a mathematical model for gas flow:

- (1) Coal seam is an infinite area in the horizontal direction.
- (2) Gas flow within coal body is in form of seepage and obeys Darcy law.
- (3) A time-dependent zone of steady flow exists within newly exposed face. Duration of steady flow is set as 24 h.
- (4) In condition of three dimensions, gas migration around the heading face can be described by the differential equation of spherical flow field. Equation (2), ignored the effect of gas adsorption, is formulated in uncoupled way to describe the steady state condition.

$$\frac{d^2 p}{dr'^2} + \frac{2}{r'} \frac{dp}{dr'} = 0 \quad (2)$$

where  $p$  is the pressure in location of radius  $r'$  of spherical flow field. With initial and boundary conditions, the pressure distribution of flow field can be obtained by Eq. (3).

$$p = p_0 - \frac{p_0 - p_a}{\frac{1}{r} - \frac{1}{R}} \left( \frac{1}{r'} - \frac{1}{R} \right) \quad (3)$$

where,  $p_0$  and  $p_a$  are the gas pressure within coal seam and atmospheric pressure respectively;  $R$  and  $r$  are the radius of gas and atmospheric pressure boundary respectively.

The gas seepage law can be written as Eq. (4).

$$v_x = -\frac{K}{\mu} \frac{dp}{dr'} \quad (4)$$

where,  $v_x$  is the gas seepage velocity;  $\mu$  is the dynamic viscosity, Pa s;  $K$  is the permeability of coal seam, m<sup>2</sup>. Gas permeability coefficient of coal seam is used to reflect the difficulty of gas flow in coal seam, in unit of m<sup>2</sup>/(MPa<sup>2</sup> d). This parameter was defined by Zhou based on the nonlinear gas flow law in the coal mass (Zhou and Lin 1999). The relationship between the gas permeability coefficient and coal permeability is as follows.

$$\lambda = \frac{K}{2\mu p_a} \quad (5)$$

where  $\lambda$  is the gas permeability coefficient of coal seam, m<sup>2</sup>/(MPa<sup>2</sup> d);

By combining the above Eqs. (3)–(5), the rate of gas flow is obtained as Eq. (6).

$$q = 2A \cdot \lambda \left( \frac{p_0 - p_a}{\frac{1}{r} - \frac{1}{R}} \right) \frac{1}{r^3} \quad (6)$$

here  $A$  is the area of gas pressure boundary in coal seam. It presents as a portion of a sphere surface and is calculated by Eq. (7).

$$A = \iint R^2 \sin \theta d\theta d\varphi \quad (7)$$

here  $\theta$  and  $\varphi$  are angular parameters of an irregular sphere. When  $\varphi = \pi$ ,  $A = \pi R^2 \int \sin \theta d\theta$ .

The gas flow field in heading face is in shape of some portion of a sphere. With the advance of heading face, the pre-existing flow field is cut down and a new flow field is formulated. Residual flow field does not change in 24 h. The gas emission of heading face within a certain time is from the integration of newly formed and residual flow fields, as shown in Fig. 5. The rate of gas flow in heading face can be transformed as Eq. (8).

$$Q_t = 2 \sum_{n=0}^n A_n(\theta_n) \cdot \lambda \left( \frac{p_0 - p_a}{\frac{1}{r_n} - \frac{1}{R_n}} \right) \frac{1}{r_n^3} \quad (8)$$

where,  $R_n$  and  $r_n$  are the radius of  $n$ th seepage field of gas and atmospheric pressure boundary respectively;  $A_n$  is the area of the  $n$ th seepage field of gas pressure boundary;  $n$  is the number of cycles of working procedures in one day.

$$A_n = \pi R_n^2 \int \sin \theta d\theta \quad (9)$$

Center position of spherical flow field is defined by Eq. (10). It is used to represent the minimum boundary of gas emission in heading face.

$$(w + y)^2 = \left( \frac{c}{2} \right)^2 + w^2 \quad (10)$$

where,  $w$  is the geometry parameter for flow field;  $y$  is the distance from loosen boundary of coal mass to coal face.

$\theta$  can be calculated on basis of the geometry parameters at head face as follows.

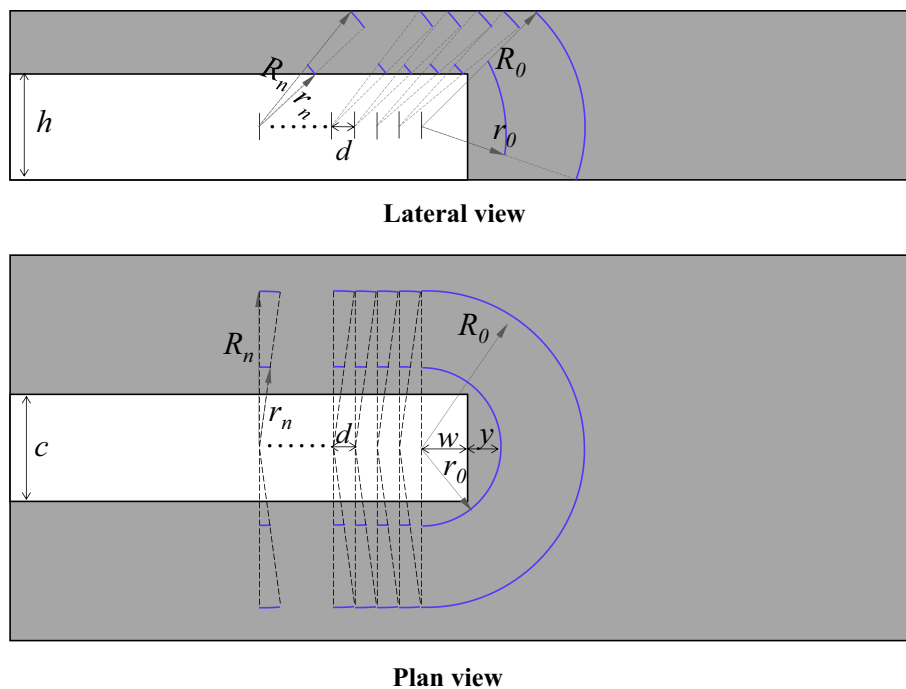


**Fig. 5** Schematic diagram of gas flow fields in heading face ( $d$  is the footage in one drifting-operation cycle;  $nd$  is the footage of tunnelling in 24 h)

$$\begin{cases} \theta_0 = \arcsin\left(\frac{2M-h}{2R_0}\right) + \arcsin\left(\frac{h}{2R_0}\right), n = 0 \\ \theta_n = \arcsin\left[\frac{d(2M-h)}{2R_n^2}\right], n \geq 1 \end{cases} \quad (11)$$

where,  $M$  is the thickness of coal seam;  $h$  is the height of roadway;  $d$  is the footage of working face.

Gas pressure distribution is related with gas flow factors, such as permeability and stress. According to findings of Connell and Si et al. (Connell 2009; Si et al. 2019), permeability of coal seam is sensitive to stress state. Stressed zone in front of heading face remains stage of pre-failure and maintains low permeability. Because of zone-based distribution of the permeability, gas pressure is also distributed zonally.  $R_0$  is determined by calculating the width of limit equilibrium zone in front of heading face (Hou and Ma 1989).

$$R_0 = \frac{hu}{2 \tan \varphi_0} \ln\left(\frac{k' \gamma' H \tan \varphi_0}{C_0} + 1\right) + w \quad (12)$$

where,  $u$  is the coefficient of horizontal pressure;  $C_0$  is the cohesion of coal;  $\varphi_0$  is the internal friction angle;  $k'$  is the coefficient of stress concentration;  $H$  is the burial depth;  $\gamma'$  is the average density of overlying strata.

$r_0$  is related to the width of loosen zone or unloading zone in front area of heading face, which is a constant

within a certain period. The empirical values, 1 to 2 m in front of coal face, can be selected.

### 2.2.2 Gas emission model of coal wall

Gas emission from coal wall can be described by a fractional attenuation model as follows (Ruban and Zaburdyaev 2011).

$$q_t = \frac{q_0}{\alpha t + 1} \quad (13)$$

where,  $q_t$  is gas flow rate of per unit area coal wall at time  $t$ ;  $q_0$  is the initial gas flow rate of coal wall;  $\alpha$  is the attenuation coefficient of gas release from coal wall.

Continuous intermittent advance of coal face results in the difference of exposure duration of coal wall spatially. The regularity of gas emission for coal wall can be revealed by an ideal roadway model, as shown in Fig. 6. The roadway is evenly divided into  $m$  segments with an unit length of  $x_0$  and an exposure time difference of  $t_0$  between segments. Gas emission of coal wall is described by Eq. (14).

$$\begin{aligned} Q''_t &= S \cdot \frac{q_0}{\alpha t_0 + 1} + S \cdot \frac{q_0}{\alpha 2t_0 + 1} \\ &+ \dots S \cdot \frac{q_0}{\alpha m t_0 + 1} \end{aligned} \quad (14)$$

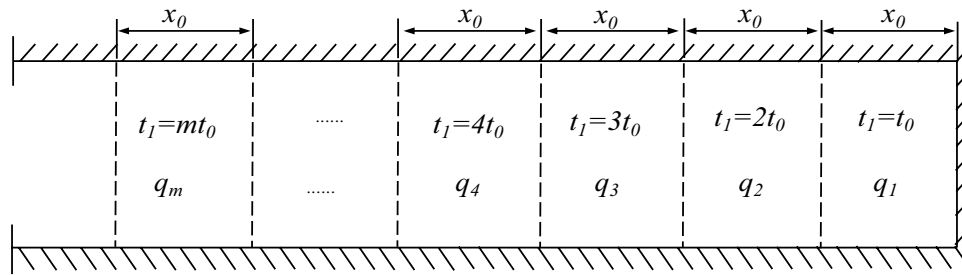


**Fig. 6** The ideal roadway model for gas emission ( $t_1$  is the exposure duration;  $q_m$  is the gas emission rate of  $m$  th segment)

$$S = 2\delta x_0 h \tag{15}$$

where,  $x_0$  is the equivalent average footage;  $h$  is the height of roadway;  $\delta$  is the coefficient related to the thickness of the coal seam  $M$  (If  $M > h$ ,  $\delta > 1$  or not  $\delta = 1$ );  $S$  is the mean exposed area of one segment of roadway.

Equation (14) is transformed into (16) by integration.

$$Q'' = Sq_0 \int_{t'_1}^{t_1} \frac{1}{\alpha t + 1} dt \tag{16}$$

where  $t_1$  is the exposure duration of roadway tunneling;  $t'_1$  represents the exposure time of excluded roadway wall. When  $t'_1 = 0$ , the quantity of gas emission from coal wall is calculated by Eq. (17) as follows.

$$Q''_t = \frac{Sq_0}{\alpha} \ln(\alpha t_1 + 1) \tag{17}$$

### 2.2.3 Gas emission model of collapsed coal

The gas release from collapsed coal is described in most general way by the exponential function (Airey 1968; Khodot 1983). The equation is expressed as follows.

$$Q'''_t = Xq'_0 e^{-\beta t_2} \tag{18}$$

$$X = kdch\gamma \tag{19}$$

where  $q'_0$  is the initial gas emission rate of collapsed coal;  $\beta$  is the attenuation coefficient of gas release from collapsed coal;  $X$  is the weight of collapsed coal in one cycle;  $k$  is the nonuniform coefficient;  $d$  is the footage in one drifting-operation cycle;  $\gamma$  is the coal density;  $t_2$  is the average stay time of collapsed coal in every cycle. The mean value of gas emissions from collapsed coal is calculated by Eq. (20).

$$Q''' = \frac{nXq'_0}{24} \int_0^{t_2} e^{-\beta t} dt \tag{20}$$

### 2.3 Gas pressure inversion model

Gas emission during roadway tunneling is complex and the dynamic process is highly dependent on operation of production processes. Gas release from every segment of roadway is attenuation with increasing duration of exposure and the head face remains higher stable outflow. All of this show the temporal and spatial characteristics. According to Eq. (8), the dimensions of gas flow field and gas pressure of coal mass determine the performance of gas emission. Gas pressure can be expressed by equation transformations, as follows.

$$p_0 = \frac{Q'}{2\lambda \sum_{n=1}^n A_n(\theta_n) \cdot \frac{R_n}{r_n(R_n - r_n)}} + p_a \tag{21}$$

An ideal state of steady gas flow in heading face means the gas pressure and sizes of flow field are relatively constant in a certain time. It is deduced that  $R_n$  and  $r_n$  are constant values within a steady flow time of 24 h. The magnitude of gas flow is governed by the cycles of working procedures. When the duration of cycles of heading face is taken by one day,  $R_0$  equals to  $R_n$  and  $r_0$  equals to  $r_n$ . Thus, gas pressure within heading face area in advance is calculated by Eq. (22).

$$p_0 = \frac{Q'(R_0 - r_0)r_0^2}{2\lambda R_0(A_0 + nA_1)} + p_a \tag{22}$$

By combining Eqs. (1), (17) and (20), gas emission rate of heading face is expressed by as follows.

$$Q' = Q - \frac{Sq_0}{\alpha} \ln\left(\frac{\alpha t_1 + 1}{24\alpha + 1}\right) - \frac{nt_2 X q'_0}{24\beta} (1 - e^{-\beta t_2}) \tag{23}$$



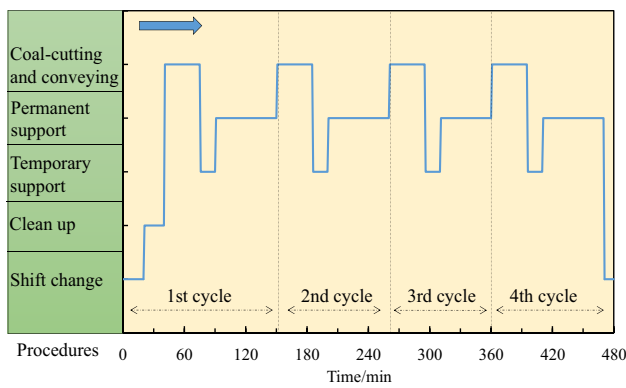


Fig. 7 Continuous cycle operation sheet in heading face

### 3 Application of dynamic inversion model in heading face

#### 3.1 Background of test field

Yuwu coal mine with annual output of 6 million tons coal is located in Qinshui coal field, China. The No. 3 coal seam, with about 6.3 m thickness, is the primary mineable coal bed. It has a high gas content, with the inclination of 3 to 11 degrees. The testing field is N1101 heading face.

Mechanized excavation technology was employed in N1101 heading face. Fresh air volumes supplied by mine secondary fan were 1580 in unit of m<sup>3</sup>/min. Figure 7 shows continuous cycle operation sheet in heading face. Working procedures include shift change, clean up, coal-cutting and conveying, temporary support and permanent support. One cycle spends about two hours. Tunneling footage in one cycle is 0.8 m.

#### 3.2 Method for key parameters in gas pressure inversion model

According to the Eqs. (19)–(21), the gas flow field boundary and the attenuation coefficient of gas release from coal

wall and collapsed coal are important parameters to obtain the gas pressure.

The  $R_0$  equals to the minimum distance of position of maximum gas pressure within coal to roadway face. The distribution of stress and gas pressure magnitude in roadway is revealed by scholars (Si et al. 2015; Yang et al. 2012; Jiang et al. 2019), as shown in Fig. 8. The zone of maintaining poor gas filtration induced by high stresses holds a high gas pressure and content. The finding that the volume of gas releasing from the sampled coal is proportional to the square root of time provides a feasible way to reveal the relation between sampling positions and the cutting test index (Bertard et al. 1970). The  $K_1$  is an index that represents gas releasing rate and content of drill cuttings, widely used for forecasting coal and gas outburst in China coal mines. For the same type of coal, the value of  $K_1$  is the reflection of gas content or pressure. Therefore, the gas flow boundary  $R_0$  can be obtained according to the sampling position with maximum values of  $K_1$ . The value of  $K_1$  can be tested by YTC10-W tester. The detailed test process is as followed. First, drill the borehole to the preset position and record the beginning time. Then, go on drilling to collect 10 g drill cuttings with particle size between 1 and 3 mm by using the sizing screen. After that, put the 10 g drill cuttings into canister of the tester and record the finish time, ensuring the duration of sampling less than 3 min. Finally, the value of  $K_1$  is measured by degassing automatically.

The attenuation coefficient of gas release from coal wall can be on-site investigated by observing gas emission when the heading face was off duty. On basis of Eqs. (11) and (15), the gas emission in this time from coal wall with the exposure time more than one day and the newly exposed coal in the heading face is estimated as follows.

$$Q_t = \frac{S'q_0}{\alpha t + 1} + \frac{Sq_0}{\alpha} \ln\left(\frac{\alpha t_1 + 1}{\alpha t + 1}\right) \tag{24}$$

where  $S'$  is the area of the heading face and calculated by  $S' = S + ch$ .

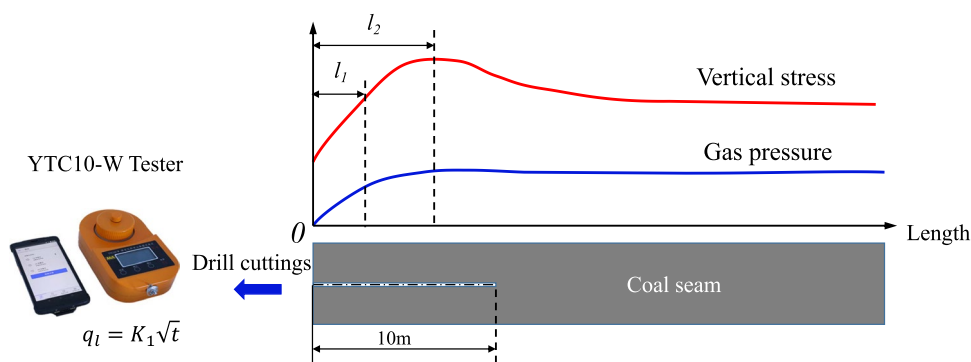


Fig. 8 Test method for gas flow boundary

While the attenuation coefficient of gas release from collapsed coal can be on-site investigated by fitting the data of gas emission rate (Eq. (16)) when the last cycle of working time was executed.

### 3.3 Verification method to gas pressure inversion model

Both gas pressure and content are used to assess the regional gas distribution (Burra and Esterle 2012). The relation between gas pressure and gas content is adopted by scholars (Tu et al. 2016; Xue et al. 2014), expressed by Eq. (25).

$$W = \frac{abp_0}{1 + bp_0} \times \frac{1}{1 + 0.31M_{ad}} \times \frac{100 - M_{ad} - A_d}{100} + V \cdot \frac{p_a}{p_0} \tag{25}$$

where *a* is maximum value of coal adsorption gas; *b* is adsorption equilibrium constant; *V* is the pore volume per unit volume of coal.

On basis of Eqs. (22) and (23), gas pressure inversion in front area of heading face is conducted by tracking the process of tunneling. The inversion gas pressure is converted into gas content and verified by the measurement of gas content.

## 4 Results

### 4.1 Gas pressure inversion

Three groups of samples during the roadway driving were tested and the distribution of the values of *K*<sub>1</sub> in front of the roadway were shown in Fig. 9. The values of *K*<sub>1</sub> in boreholes at 5 m in front of the roadway face reached the maximum, and that at 1 m remained a relatively small value. Drill

cuttings sampled more than 5 m in borehole showed the varied values of *K*<sub>1</sub> but less than the maximum. When the sample retrieval time was longer, lost gas estimation may cause the potential error inherent. Therefore, the results of drill cuttings close to borehole bottom showed obvious changes. Coal close to the roadway face tends to release more gas, but there exists an extreme distance in coal seam where the gas content is closed to original state. According to the Eqs. (10) and (12), theoretical value of *R*<sub>0</sub> is 8.2 m (Parameter values is chosen by referring to engineering background. *H* is 620 m; *u* is 0.8; *k'* is 1.5; *C*<sub>0</sub> is 1.3 MPa; *φ*<sub>0</sub> is 41°; *w* is 3.2 m). Location of maximum value *K*<sub>1</sub>, 5 m in front of coal face, fits the theoretical value. And location of smaller value *K*<sub>1</sub>, 1 m in front of coal face, fits the empirical results of *r*<sub>0</sub>. Combined with theory analysis and on-site measurement values, the *R*<sub>0</sub> and *r*<sub>0</sub> are taken as 8.2 m and 4.2 m, respectively.

Figure 10a showed the downtrend of gas emission in the roadway when the heading face stopped driving from Aug. 24 to Sep. 01. At this time, the gas emission was composed of the one from coal wall (over one day) and the newly exposed coal in the heading face. Based on the data of gas emission in the roadway from Aug. 24th to Sep. 1st and Eq. (24), the fitting curve was obtained and shown in Fig. 10b. The fitting result indicates that the attenuation coefficient *α* equals to 0.61 and the initial gas flow rate *q*<sub>0</sub> equals to 0.018 m<sup>3</sup>/(m<sup>2</sup> min).

During the excavation, the collapsed coal also contributes to the gas emission and the volumes can increase as the increase of output coal. Figure 11a showed the change of gas concentration of return air versus a specific point in time. The magnitude of gas concentration was associated with state of working time and downtime. When the last cycle of working time was executed, the data of gas emission rate were used to fit the attenuation regularity, as shown in

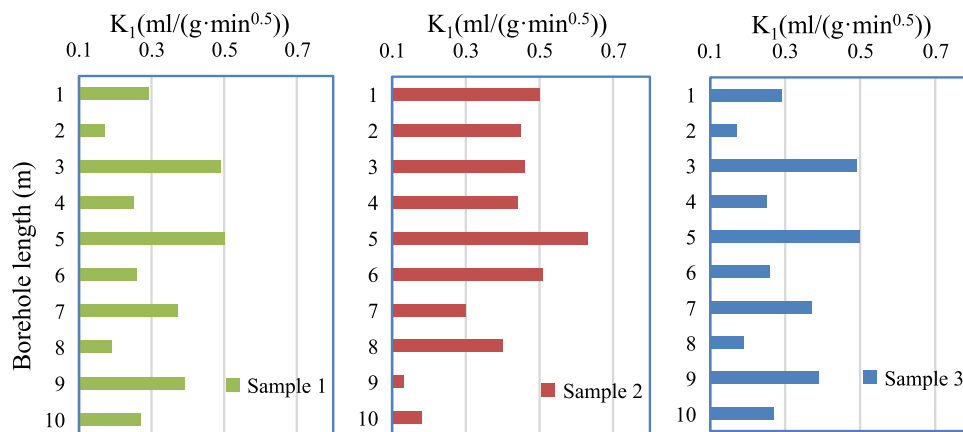
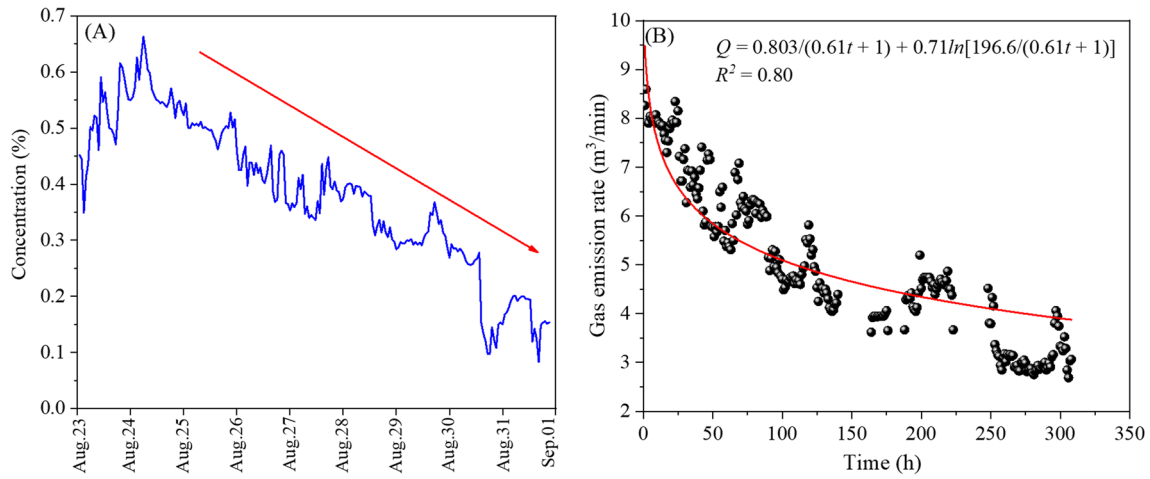
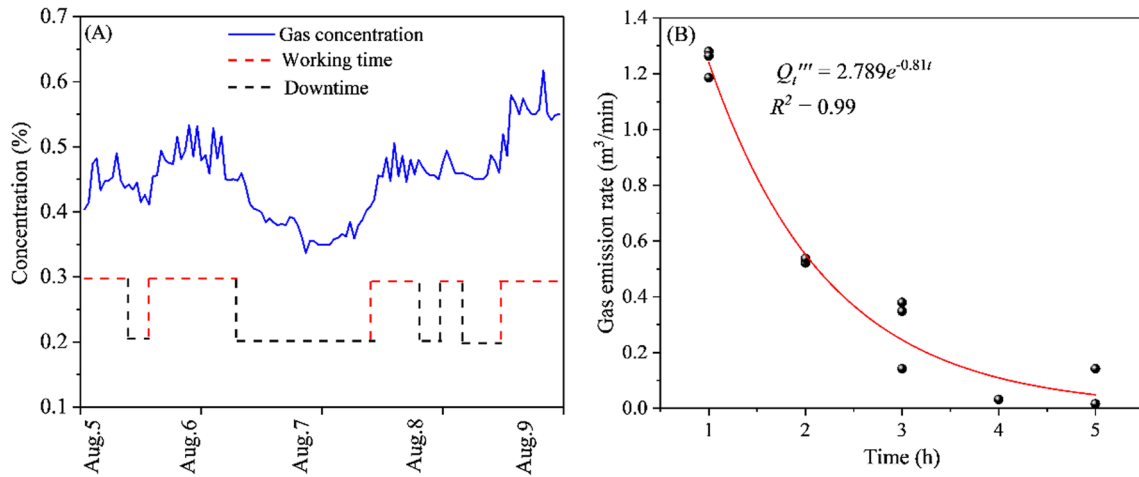


Fig. 9 Results of *K*<sub>1</sub> distributions of borehole drilling cuttings





**Fig. 10** Attenuation regularity of gas emission from coal wall (a Gas concentration of return air when the heading face off duty; b Fitting curve for gas emission)



**Fig. 11** Attenuation regularity of gas emission from collapsed coal (a Variation of gas concentration during roadway driving; b Fitting curve of gas emission from collapsed coal)

Fig. 11b. The attenuation coefficient  $\beta$  equals to 0.81 and the initial gas emission rate  $q_0'$  equals to  $0.105 \text{ m}^3/(\text{t min})$ . Combined the above analysis with the field data, the parameters shown in Table 1 were used for gas pressure inversion.

### 4.2 Model validation

The volumes of gas emission from the heading face, coal wall and collapsed coal varied with the advancement of heading face. Based on the Table 1 and Eqs. (17), (20), (23), the volume of gas emission from different sources were calculated. Figure 12 shows the percentage of gas emission volume from different sources. The percentage of gas emission volume from the heading face ranges from 7% to 47%, and that from coal wall and collapsed coal ranges from 47%

to 82% and 2% to 11%, respectively. The percentage of gas emission volume from collapsed coal is the smallest, which is related to the continuous output of coals. The percentage of gas emission volume from coal wall is the biggest, which is related to the added coal wall with the advancement of coal face.

According to the calculated volume of gas emission from the heading face and Eqs. (19), (20), the results of gas pressure inversion hour by hour in front area of heading face are shown in Fig. 13. Records of working conditions of heading face are shown in Table 2. From Figs. 13a, c, e, the gas pressure varied with the gas emission rate per hour. Due to the gas pressure obtained in the heading face, the sudden increase of gas emission is mainly induced by the gas flooding of collapsed coal and the newly exposed coal in the

**Table 1** Parameters for gas pressure inversion

Parameter	Value
Gas permeability coefficient, $m^2/(MPa^2 d)$	0.421
Underground atmospheric pressure, $p_a$ (MPa)	0.1
Radius of gas pressure boundary, $R_0$ (m)	8.2
Radius of atmospheric pressure boundary, $r_0$ (m)	4.2
Thickness of coal seam, $M$ (m)	6
Initial gas flow rate of coal wall, $q_0$ ( $m^3/(m^2 \cdot h)$ )	0.018
Gas attenuation coefficient of coal wall, $\alpha$	0.61
Height of roadway, $h$ (m)	3.8
Width of roadway, $c$ (m)	5.4
Coefficient related to $M$ , $\delta$	1.5
Initial gas emission rate of collapsed coal, $q_0^1$ , $m^3/(th)$	0.105
Gas attenuation coefficient of collapsed coal, $\beta$	0.81
Footage in one drifting-operation cycle, $d$ (m)	0.8
Coal density, $\gamma$ ( $t/m^3$ )	1.43
Nonuniform coefficient of collapsed coal, $k$	1.3
Pore volume, $V$ ( $m^3/t$ )	0.024
Maximum value of coal adsorption gas, $a$ ( $m^3/t$ )	33.9
Adsorption equilibrium constant, $b$ ( $MPa^{-1}$ )	0.855
Moisture content on air-dried basis, $M_{ad}$ (%)	0.97
Ash content on air-dried basis, $A_{ad}$ (%)	15.81

heading face. While the Fig. 12 shows that the percentage of gas emission volume from the collapsed coal is smaller than that from the heading face. Therefore, the gas pressure is directly reflected by the rate of gas emitting from the newly exposed coal in the heading face.

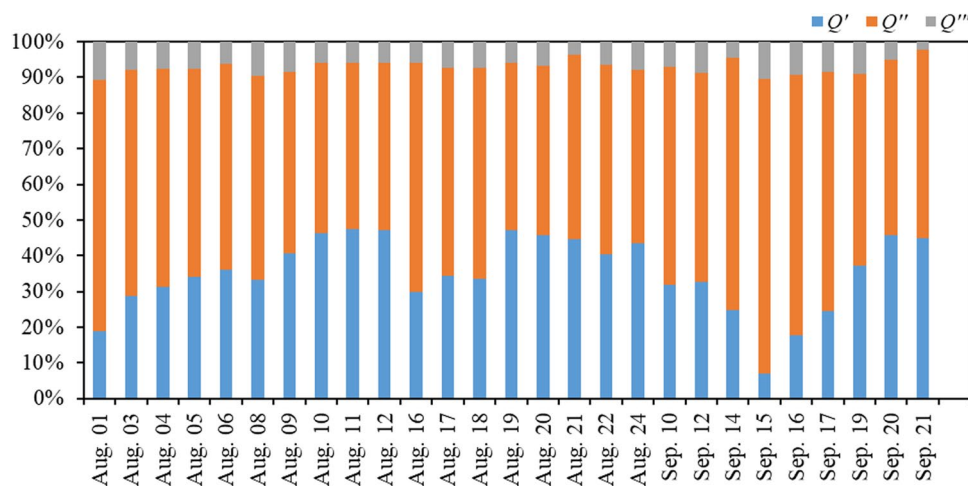
After obtaining the inversion gas pressure, the gas pressure is converted into gas content based on Eq. (25). The theoretical result and experimental result of gas content was compared in Figs. 13b, d, f, which was used to verify the gas pressure inversion model. The test results of gas content

on Aug. 5th, Aug. 17th, Sep. 12th, 2015 are 9.61, 9.84 and 9.39  $m^3/t$ , while the average values of theoretical results of gas content on Aug. 5th, Aug. 17th, Sep. 12th, 2015 are 9.42, 9.45 and 9.06  $m^3/t$ , with the absolute error about 2%, 3.9%, 3.5%. Compared with the experiment results, the fluctuation trend of theoretical results is within a tolerable level (Figs. 13b, d, f). The corresponding absolute errors between the theoretical result in every hour and test result are 0.8%–21.1%, 0.4%–21.7%, 0.6%–33% on Aug. 5th, Aug. 17th, Sep. 12th, respectively. Most of absolute errors between the theoretical result in every hour and test hour are lower than 20%, which proves the rationality of the gas pressure inversion model.

## 5 Discussion

### 5.1 Analysis of inversion results

According to the average value of gas emission rate in one day, the continue gas pressure inversion is conducted in days. Figure 14 shows the continuous inversion results of gas pressure with daily footage. The gas pressure varied with the advancement of heading face and reached the maximum of 1.15 MPa and the minimum of 0.19 MPa (Fig. 14a). The gas emission rate is related to the gas content of coal seam with the maximum of 12.54  $m^3/t$  and the minimum of 3.47  $m^3/t$  (Fig. 14b). A certain correlation appears between drifting footage per day and gas pressure. The continuous and maximum drifting footage per day leads to a high-level of gas emission associated with the maximum gas pressure in front area of heading face, which indicates that decreasing the construction speed is beneficial to the decrease of gas pressure in front area of heading face, as well as the gas content.

**Fig. 12** Percentage of gas emission volume from different sources

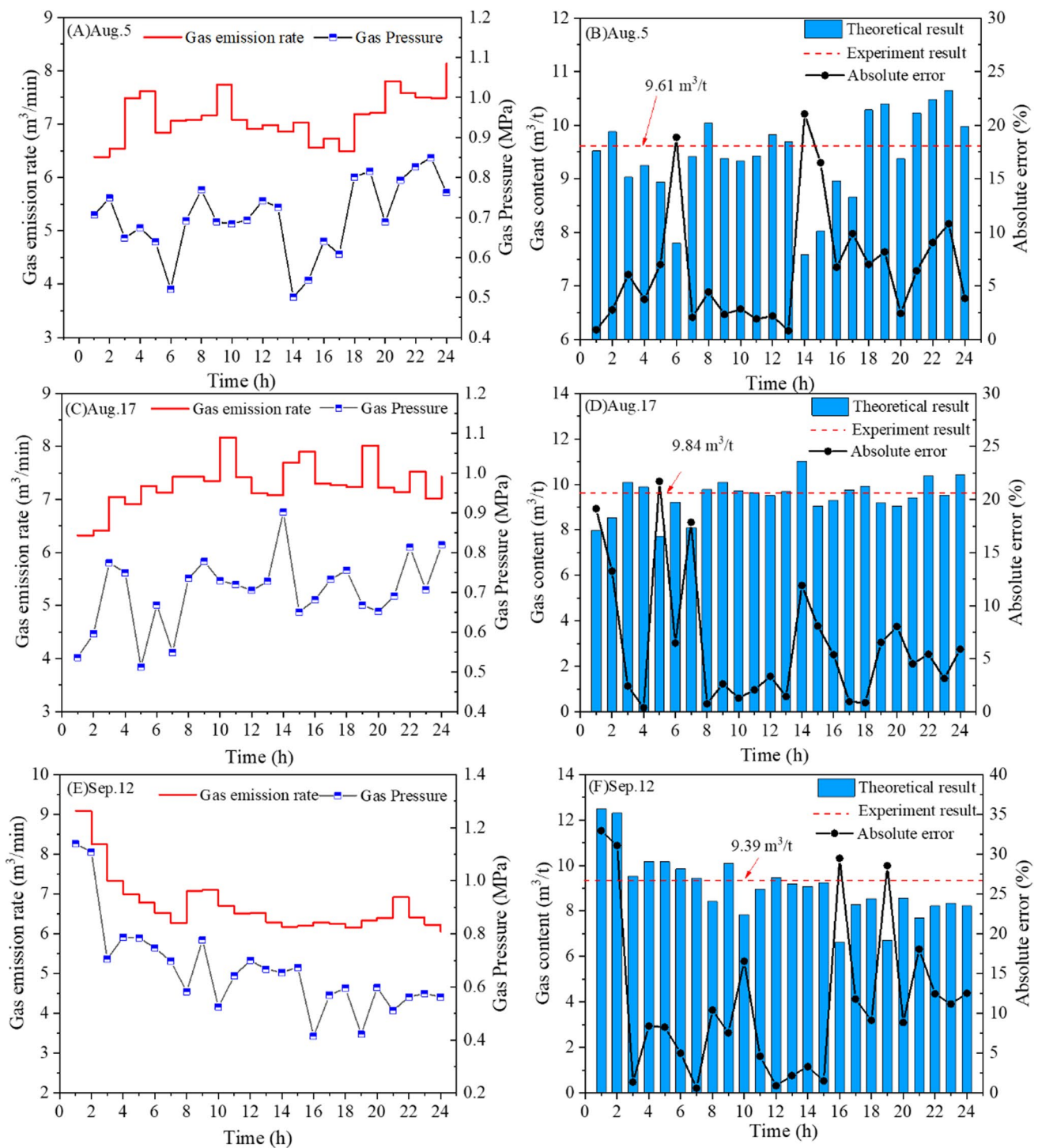


Fig. 13 Inversion results and gas content verification

Figure 15 presents the effects of different influencing parameters on the gas pressure inversion. The radius of gas pressure boundary  $R_1$  largely influences the gas pressure near the heading face, whilst the radius of atmospheric pressure boundary  $r_1$  has minimal effects. This is because the

$R_1$  is positively correlated with the scope of gas flow field in coal seam.  $r_1$  is related to the distance of gas flow and produces a limited impact on gas flow rate. From Fig. 15b, the variation of gas permeability coefficient  $\lambda$  can induce the violent fluctuation of gas pressure in coal seam. Large gas

**Table 2** Records of working conditions of heading face

Date	Drifting footage (m)	Number of cycles	Tons of output (t)	Average daily gas emission ( $m^3/min$ )
Aug. 5	5.6	7	164	7.1
Aug. 17	5.4	6	158	7.3
Sep. 12	6.3	7	184	6.7

emission rate  $Q$  with a lower value of  $\lambda$  indicates a higher value of gas pressure.  $\lambda$  is not the laboratory result but measured on-site by observing gas flow rate of the crossing borehole in coal seam according to China standard (National Mine Safety Administration 2019).  $R_0$ ,  $r_0$  and  $\lambda$  are mainly

influenced by burial conditions of mining area. Within a certain region, the aforementioned parameters can be considered as the constant, since the gas pressure inversion is conducted in condition of the same excavating technology, stable burial depth and less than 24 h after tunneling.

### 5.2 Implication to coal and gas outburst

In the coal mines, the sudden increase of gas emission can be an indicator for warning the coal and gas outburst. While the gas pressure is one of the most important indexes to evaluate the coal and gas outburst. In this work, the gas emission rate can be converted to gas pressure by the gas pressure inversion method. The inversion method is on basis of

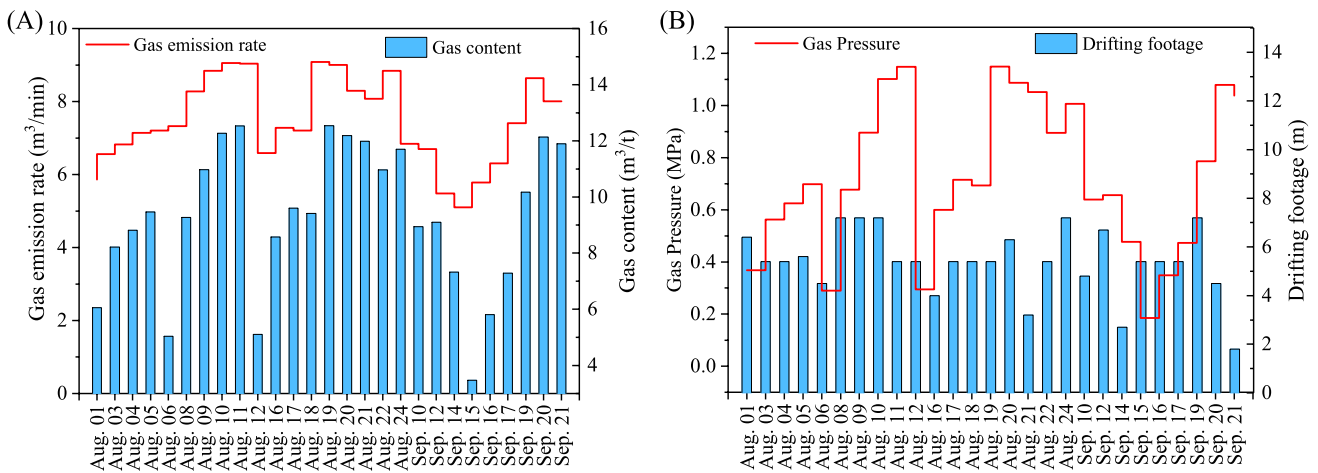


**Fig. 14** Continuous inversion results of gas pressure in 28 days

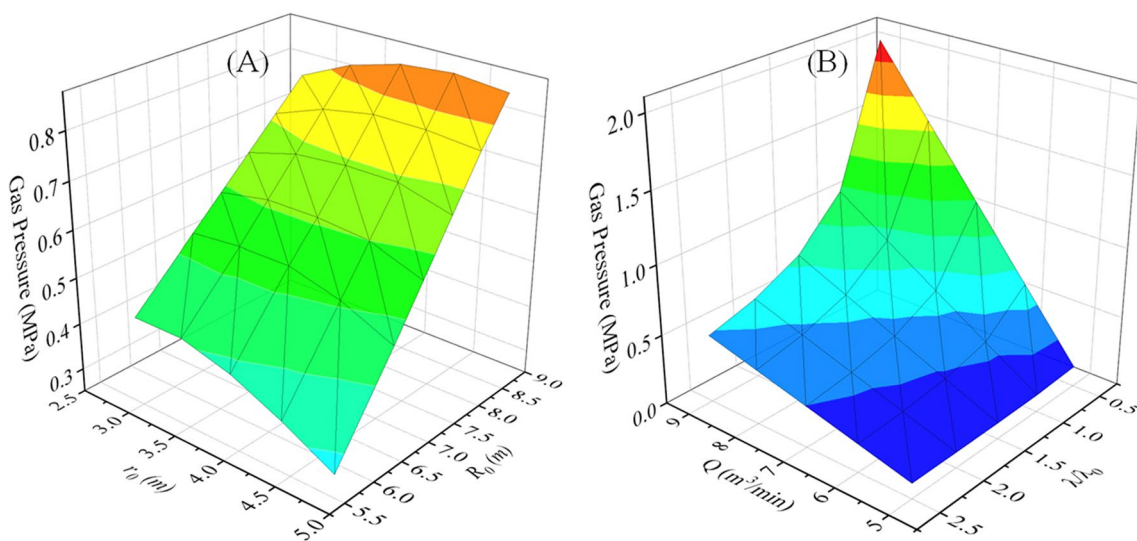


**Fig. 15** Influences of **a**  $r_1$  and  $R_1$  and **b**  $\lambda$  and  $Q$  on gas pressure close to a development face ( $\lambda_0$  is initial value of gas permeability coefficient of coal seam)

a hypothesis that the gas migration within newly exposed coal in the heading face is steady flow in a certain time (24 h in paper). According to the inversion results, the variation trend of gas pressure is similar with that of gas emission rate, which indicates that the inversion gas pressure can be an index to assess and warn the coal and gas outburst. Besides, the inversion results can verify that the speedy excavation can increase the risk of coal and gas outburst. But, if the heading face is off work or daily drifting footage is zero, the accuracy of the results may be compromised. Even so, this method has the potential to improve the means of monitoring and warning coal and gas outburst in the roadway.

### 6 Conclusions

On premise of the hypothesis that a time-dependent zone of steady flow exists within newly exposed face, a novel inversion model of gas pressure in front area of the heading face was established and verified. The main conclusions drawn from the investigations are summarized below:

- (1) The gas flow in front area of heading face is the integration of several partial-sphere flow fields. One day duration of steady flow for model is verified by on-site application.
- (2) The percentage of gas emission from heading face, coal wall and collapsed coal was obtained and showed that variations of gas emission from heading face imply the variations of gas pressure and content. The inversion results prove that speedy excavation can increase the risk of gas disaster.
- (3) A technical route for gas pressure inversion in front area of heading face is produced, including theoretical basis, key parameters investigation and inversion method. It has the potential to improve the means of gas disaster monitoring and forecasting in roadway.

### Appendix

Gas permeability coefficient of coal seam, in unit of  $m^2/(MPa^2 \cdot d)$ , is calculated follow the flowchart, as is shown in Fig. 16. Crossing hole is employed to drill into coal seam from roadway. The borehole is sealed and equipped with a pressure gauge until the variation of gas pressure is stable. After pressure gauge is removed, the gas flow in underground atmosphere is observed with flow-meter within a few days. The stable rate of flow  $Q_m$  is used to calculate the permeability coefficient.  $L$  is the borehole length in coal seam.  $r_m$  is the diameter of borehole. On basis of the inputted parameters, the value of  $\lambda$  is obtained by iteration.

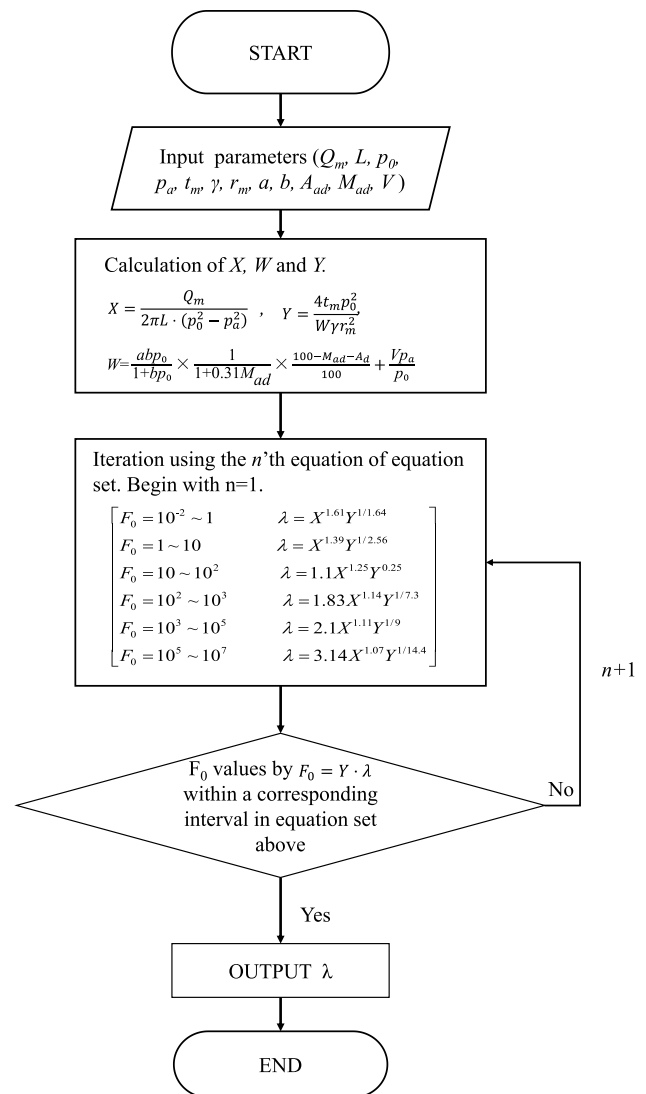


Fig. 16 Flowchart of calculation of gas permeability coefficient of coal seam

**Acknowledgements** This work is financially supported by the General Program of National Natural Science of China (52174187) and the State Key Program of National Natural Science of China (52130409).

**Funding** General Program of National Natural Science of China (52174187); State Key Program of National Natural Science of China (52130409).

### Declarations

**Conflict of interest** The authors declare no conflict of interest.

**Open Access** This article is licensed under a Creative Commons Attribution 4.0 International License, which permits use, sharing, adaptation, distribution and reproduction in any medium or format, as long as you give appropriate credit to the original author(s) and the source, provide a link to the Creative Commons licence, and indicate if changes were made. The images or other third party material in this article are included in the article’s Creative Commons licence, unless indicated



otherwise in a credit line to the material. If material is not included in the article's Creative Commons licence and your intended use is not permitted by statutory regulation or exceeds the permitted use, you will need to obtain permission directly from the copyright holder. To view a copy of this licence, visit <http://creativecommons.org/licenses/by/4.0/>.

## References

- Airey EM (1968) Gas emission from broken coal. An experimental and theoretical investigation. *Int J Rock Mech Min Sci Geomech Abstr* 5:475–494
- An F, Cheng Y, Wu D, Li W (2011) Determination of coal gas pressure based on characteristics of gas desorption. *J Min Saf Eng* 28(1):81–85
- An FH, Cheng YP, Wang L, Li W (2013) A numerical model for outburst including the effect of adsorbed gas on coal deformation and mechanical properties. *Comput Geotech* 54:222–231
- Bertard C, Bruyet B, Gunther J (1970) Determination of desorbable gas concentration of coal (direct method). *Int J Rock Mech Min* 7:43–65
- Burra A, Esterle J (2012) Gas distribution and geology: A Hunter Valley example. In: *Proceedings of the 38th symposium on the advances in the study of the sydney Basin, Hunter Valley, Australia*
- Ceglarska-Stefanska G, Zarębska K (2005) Sorption of carbon dioxide–methane mixtures. *Int J Coal Geol* 62:211–222
- Connell LD (2009) Coupled flow and geomechanical processes during gas production from coal seams. *Int J Coal Geol* 79:18–28
- Czerw K (2011) Methane and carbon dioxide sorption/desorption on bituminous coal—experiments on cubicoid sample cut from the primal coal lump. *Int J Coal Geol* 85:72–77
- Dougherty HN, Özgen Karacan C (2011) A new methane control and prediction software suite for longwall mines. *Comput Geosci-UK* 37:1490–1500
- Gerami A, Mostaghimi P, Armstrong RT, Zamani A, Warkiani ME (2016) A microfluidic framework for studying relative permeability in coal. *Int J Coal Geol* 159:183–193
- Hou C, Ma N (1989) Stress in in-seam roadway sides and limit equilibrium zone. *J Chin Coal Soc* 14:21–29
- Hou S, Wang X, Wang X, Yuan Y, Pan S, Wang X (2017) Pore structure characterization of low volatile bituminous coals with different particle size and tectonic deformation using low pressure gas adsorption. *Int J Coal Geol* 183:1–13
- Jiang Y, Zhou H, Lu J, Gao Y, Zhang C, Chen J (2019) Analysis of stress evolution characteristics during TBM excavation in deep buried tunnels. *Bull Eng Geol Env* 78:5177–5194
- Karacan CO, Ruiz FA, Cote M, Phipps S (2011) Coal mine methane: a review of capture and utilization practices with benefits to mining safety and to greenhouse gas reduction. *Int J Coal Geol* 86:121–156
- Khodot VV (1983) Calculation of the gas release from a sudden ejection of coal and gas. *Sov Min* 19:432–436
- Khodot VV, Isaeva RN, Krupenya VG (1972) Calculation of the fall in gas pressure during degassing of thin coal seams by large-diameter boreholes. *Sov Min* 8:291–295
- Khristianovich SA, Kovalenko YF (1988) Measurement of gas pressure in coal seams. *Sov Min* 24:181–199
- Kurlenya MV, Shilova TV, Serdyukov SV, Patutin AV (2014) Sealing of coal bed methane drainage holes by barrier screening method. *J Min Sci* 50:814–818
- Liu Q, Wang E, Kong X, Li Q, Hu S, Li D (2018) Numerical simulation on the coupling law of stress and gas pressure in the uncovering tectonic coal by cross-cut. *Int J Rock Mech Min* 103:33–42
- Ma YK, Nie BS, He XQ, Li XC, Meng JQ, Song DZ (2020) Mechanism investigation on coal and gas outburst: an overview. *Int J Miner Metall Mater* 27:872–887
- National mine safety administration (2019) MTT 1173–2019 Measuring method for gas permeability coefficient of coal seam—radial flow method. Beijing, China
- Peng S, Chen H, Yang R, Gao Y, Chen X (2006) Factors facilitating or limiting the use of AVO for coal-bed methane. *Geophysics* 71(4):C49–C56
- Ruban AD, Ziburdaev VS (2011) Parametrization procedure for coal bed degassing. *J Min Sci* 47:267–275
- Shi SZ, Guo JC, Gu JY, Li YY, Liu ZY, Feng J (2018) Exploration research on 2011ZX\_CC\_01 well blowout in east five panel of sihe mine. *J Chin Coal Soc* 43(11):3187–3195
- Si G, Jamnikar S, Lazar J, Shi J-Q, Durucan S, Korre A, Zavšek S (2015) Monitoring and modelling of gas dynamics in multi-level longwall top coal caving of ultra-thick coal seams, part I: borehole measurements and a conceptual model for gas emission zones. *Int J Coal Geol* 144–145:98–110
- Si G, Durucan S, Shi JQ, Korre A, Cao W (2019) Parametric analysis of slotting operation induced failure zones to stimulate low permeability coal seams. *Rock Mech Rock Eng* 52:163–182
- Tu QY, Cheng YP, Guo PK, Jiang JY, Wang L, Zhang R (2016) Experimental study of coal and gas outbursts related to gas-enriched areas. *Rock Mech Rock Eng* 49:3769–3781
- Valliappan S, Zhang W (1996) Numerical modelling of methane gas migration in dry coal seams. *Int J Numer Anal Met* 20:571–593
- Wang H, Xian X, Yin G, Zhang R, Yang J, Tang J (1999) Investigation of analytic method for coalbed gas pressure in high temperature and deeply mining mines. *J Chin Coal Soc* 24(3):280–283
- Wang L, Cheng YP, Wang L, Guo PK, Li W (2012) Safety line method for the prediction of deep coal-seam gas pressure and its application in coal mines. *Saf Sci* 50:523–529
- Wang EY, Liu SQ, Gao RB, Liu ZJ (2017) Transient electromagnetic exploration-based experiment on the relationship between the level of gas content and apparent resistivity in high rank coal seam. *Coal Geol Explor* 45(6):149–153
- Wang L, Lu Z, Chen DP, Liu QQ, Chu P, Shu LY, Ullah B, Wen ZJ (2020a) Safe strategy for coal and gas outburst prevention in deep-and-thick coal seams using a soft rock protective layer mining. *Saf Sci* 129:104800
- Wang H, Wang EY, Li ZH, Wang XR, Zhang QM, Li B, Ali M (2020b) Study on sealing effect of pre-drainage gas borehole in coal seam based on air-gas mixed flow coupling model. *Process Saf Environ* 136:15–27
- Wang H, Wang E, Li Z, Shen R, Liu X (2021) Study and application of a new gas pressure inversion model in coal seam while drilling based on directional drilling technology. *Fuel* 306:121679
- Wu D, Cheng Y, An F (2006) Determination of gas pressure and gas content based on residual gas quantity of coal sample. *J Min Saf Eng* 28(2):315–318
- Xue S, Yuan L, Wang YC, Xie J (2014) Numerical analyses of the major parameters affecting the initiation of outbursts of coal and gas. *Rock Mech Rock Eng* 47:1505–1510
- Yang W, Lin BQ, Zhai C, Li XZ, An S (2012) How in situ stresses and the driving cycle footage affect the gas outburst risk of driving coal mine roadway. *Tunn Undergr Sp Technol* 31:139–148
- Zhang K, Sun K, Yu BY, Gamage RP (2016) Determination of sealing depth of in-seam boreholes for seam gas drainage based on drilling process of a drifter. *Eng Geol* 210:115–123
- Zhang JG, Zhai C, Zhong C, Xu JZ, Sun Y (2019) Investigation of sealing mechanism and field application of upward borehole self-sealing technology using drill cuttings for safe mining. *Saf Sci* 115:141–153



- Zhang J, Zhang Y, Wang J, Wen X (2021) Prediction of gas pressure in thin coal seams in the Qinglong coal mine in Guizhou province, China. *J Petrol Explor Product Technol* 11:4075–4086
- Zhao Y, Hu Y, Zhao B, Yang D (2004) Nonlinear coupled mathematical model for solid deformation and gas seepage in fractured media. *Transp Porous Med* 55:119–136
- Zhao JL, Xu H, Tang DZ, Mathews JP, Li S, Tao S (2016) Coal seam porosity and fracture heterogeneity of macrolithotypes in the Hancheng Block, eastern margin, Ordos Basin, China. *Int J Coal Geol* 159:18–29
- Zhao Y, Sun Y, Liu S, Chen Z, Yuan L (2018) Pore structure characterization of coal by synchrotron radiation nano-CT. *Fuel* 215:102–110
- Zhou A, Wang J, Wang K, Elsworth D, Zhang M (2020) A novel double-doped polymer-modified cement-based sealant to enhance borehole seals and reduce methane emissions. *Greenh Gas* 10:313–330
- Zhou SN, Lin BQ (1999) *The theory of gas flow and storage in coal seams*. Beijing, China

**Publisher's Note** Springer Nature remains neutral with regard to jurisdictional claims in published maps and institutional affiliations.